



# Global distribution of winter lightning: a threat to wind turbines and aircraft

Joan Montanyà<sup>1</sup>, Ferran Fabró<sup>1</sup>, Oscar van der Velde<sup>1</sup>, Víctor March<sup>2</sup>, Earle Rolfe Williams<sup>3</sup>, Nicolau Pineda<sup>4</sup>, David Romero<sup>1</sup>, Glòria Solà<sup>1</sup>, and Modesto Freijo<sup>1</sup>

<sup>1</sup>Department of Electrical Engineering, Universitat Politècnica de Catalunya, Terrassa (Barcelona), 08222, Spain

<sup>2</sup>Gamesa Innovation & Technology, Sarriguren (Navarra), Spain

<sup>3</sup>Massachusetts Institute of Technology, Cambridge, MA, USA

<sup>4</sup>Meteorological Service of Catalonia, Barcelona, Spain

*Correspondence to:* Joan Montanyà (montanya@ee.upc.edu)

Received: 30 October 2015 – Published in Nat. Hazards Earth Syst. Sci. Discuss.: 19 January 2016

Revised: 31 March 2016 – Accepted: 31 May 2016 – Published: 21 June 2016

**Abstract.** Lightning is one of the major threats to multi-megawatt wind turbines and a concern for modern aircraft due to the use of lightweight composite materials. Both wind turbines and aircraft can initiate lightning, and very favorable conditions for lightning initiation occur in winter thunderstorms. Moreover, winter thunderstorms are characterized by a relatively high production of very energetic lightning. This paper reviews the different types of lightning interactions and summarizes the well-known winter thunderstorm areas. Until now comprehensive maps of global distribution of winter lightning prevalence to be used for risk assessment have been unavailable. In this paper we present the global winter lightning activity for a period of 5 years. Using lightning location data and meteorological re-analysis data, six maps are created: annual winter lightning stroke density, seasonal variation of the winter lightning and the annual number of winter thunderstorm days. In the Northern Hemisphere, the maps confirmed Japan to be one of the most active regions but other areas such as the Mediterranean and the USA are active as well. In the Southern Hemisphere, Uruguay and surrounding area, the southwestern Indian Ocean and the Tasman Sea experience the highest activity. The maps provided here can be used in the development of a risk assessment.

## 1 Introduction

Storms and lightning differ from one geographic area to another. In Europe, lightning activity is concentrated during the “warm season” since it is related to solar heating and availability of atmospheric water vapor (e.g., Poelman et al., 2016; Anderson and Klugmann, 2014). Poelman et al. (2016) found that winter months account only for 3% of the annual lightning in Europe. Although globally lightning activity associated to winter thunderstorms is relatively low compared with summer thunderstorms, these storms can produce very energetic lightning events and a large amount of damage (e.g., Yokoyama et al., 2014). Moreover, winter storms present the most favorable conditions for the initiation of upward lightning flashes from sensitive tall structures such as wind turbines (e.g., Montanyà et al., 2014a) and for flying aircraft (e.g., Wilkinson et al., 2013). A recent study by Honjo (2015) of a sample of 506 lightning currents to wind turbines in Japan concludes that winter lightning currents tend to feature longer duration currents, often bipolar, and that some particular wind turbines can be struck by lightning repeatedly in short periods of time. From the data, in about 5% of the cases the charge transferred by lightning exceeded 300 C. Wang and Takagi (2011) analyzed a sample of 100 records and summarized that 67.6% of the cases presented negative polarity, 5.9% presented positive polarity and 26.5% presented bipolar currents. In that study they also found that about a 50% of the cases were self-initiated by the wind turbine and approximately the same percentage of flashes were initiated by other lightning activity. The au-

thors noted that active thunderstorms produced more induced lightning than those storms with lower lightning activity. Additionally, Wang and Takagi (2011) noted that strong wind conditions common in winter storms may favor upward lightning initiation.

Regarding aircraft, Murooka (1992) showed how lightning strikes to airplanes typically occur at lower altitudes during winter compared to summer. Gough et al. (2009) identified that 40 % of the studied lightning events involving airplanes occurred during the “cold season”, which is not the period of the most frequent thunderstorm activity. Moreover, Wilkinson et al. (2013) concluded that because the lightning strike rate to helicopters in the North Sea during winter was much higher than expected, the presence of a helicopter actually triggers lightning. This phenomena presents a significant safety risk to helicopters doing operations under these conditions.

The main goal of this paper is to present a global map of winter lightning occurring in cold air mass thunderstorms (our criterion is  $< -10^{\circ}\text{C}$  at 700 hPa), and we summarize the lightning interactions related to winter storms. This is an important aspect which can vary according to the climatology of the thunderstorms for a particular area. Additionally, a global overview of winter storms is presented as well as the resulting lightning maps that have been computed from global lightning data. These maps will provide a tool to identify risk areas of winter lightning when performing risk assessment.

## 2 Lightning interactions

Risk assessment can only be done effectively with a complete understanding of the interactions between lightning and the struck object. Wind turbines are tall structures and thus can both receive downward and initiate upward lightning. In the case of an aircraft lightning is initiated in a bidirectional way (positive and negative leaders) from itself when flying in or beneath a thunderstorm. In this section we review the types of lightning related to wind turbines and aircraft. We do this because the mechanisms of lightning interaction with wind turbines and aircraft can differ from winter thunderstorms to summer storms (storms associated with deeper convection).

First of all, downward lightning to wind turbines (Fig. 1a) can be more common in relation to deep convective situations (e.g., summer storms in the Northern Hemisphere and tropical storms). Downward lightning is the most frequent type of lightning and is also a threat to wind turbines and aircraft. The number of downward lightning events to a particular wind turbine will depend on the exposure of the turbine and the regional ground flash density.

In the case of upward lightning two situations are distinguished regarding the triggering of an upward leader from the turbine: induced (Fig. 1b and c) and self-initiated (Fig. 1d). We use the term “induced lightning” when it is related to the

occurrence of another lightning flash which does not strike the turbine. In the case of induced upward flashes, a nearby cloud-to-ground (CG) flash or an intra-cloud (IC) flash can provide the conditions for the inception of an upward leader. Upward induced lightning is more likely to occur during warm season storms because of the high occurrence of lightning. Figure 1b and c depict that situation. Under a thunderstorm, due to the intense electric fields produced by cloud charges, wind turbines can produce corona discharges. By means of corona, electric space charge is produced (positive for a typical dipole or tripolar charge structure as discussed in Williams, 1989). As indicated by Montanyà et al. (2014a) this space charge screens the electric field at the turbine tip, thereby preventing the initiation of a leader. In order to produce a stable leader, the field needs to increase at the tip of turbine (Bazelyan and Raizer, 1998). This increase of the electric field can be produced thanks to the fast neutralization of charge produced in a CG (e.g., Warner et al., 2012 and Montanyà et al., 2014b) or an IC flash. Because of the slow ion mobility of the space charge at the tip of the turbine, the electric field is not screened and it is increased. In the case of wind turbines, the most favorable conditions for induced triggered lightning will be the case of a fast and large charge neutralization in nearby CG and IC flashes and with enhanced electric fields due to the terrain height (close to the cloud charge) and orography (e.g., on mountain peaks).

A more favorable situation for self-initiated upward lightning is present in winter thunderstorms (Fig. 1d). As a result of the dependence of the electrification processes on temperature (e.g., Takahashi, 1984, and Saunders et al., 2006), the cloud charges are located closer to the ground in winter. However, even with the lower height of the cloud charges, winter storms are not prolific generators of downward lightning (Michimoto, 1993; López et al., 2012; Bech et al., 2013; Hunter et al., 2001). That might be explained because the presence of opposite polarity charge under the mid-level charge region is necessary to initiate a leader in the cloud (Krehbiel et al., 2008). In the case of winter storms in Europe, Montanyà et al. (2007) showed that, because of the low altitude of the freezing level (even at the ground), the lower positive charge center in the cloud might not be accumulated and then downward lightning may not be initiated. However, prominent objects on the ground or at mountain tops have favorable conditions to initiate an upward leader (e.g., Warner et al., 2014).

Another special situation characterized by energetic lightning is produced in relation to the stratiform regions of mesoscale convective systems (MCSs) (Fig. 1e). MCSs are also common in winter storm structures (e.g., Mediterranean storms). MCSs can present a higher percentage of positive CG lightning activity and higher peak currents than produced by cellular summer storms (e.g., MacGorman and Morgenson, 1998). It is well known that intense +CG flashes occur in the stratiform regions of MCSs, which also excite sprites in the mesosphere (e.g., Lyons, 1996; Williams et al., 2010;

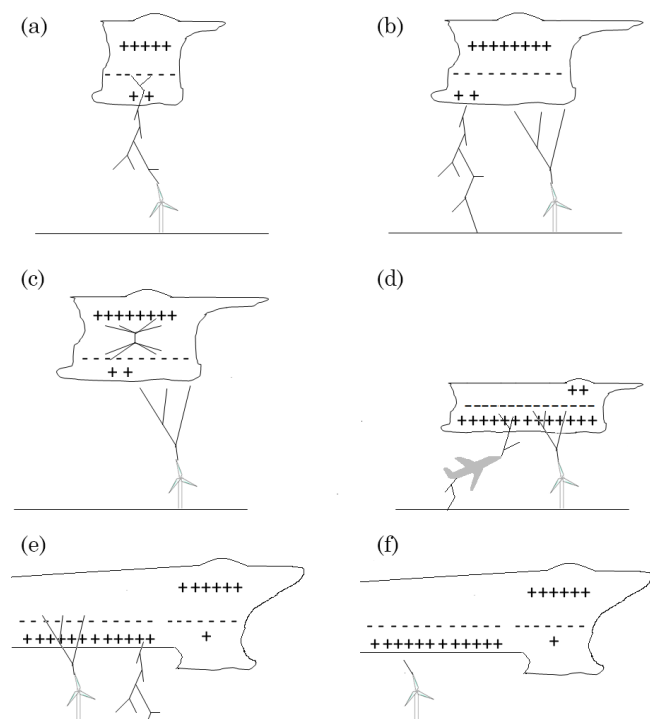


**Figure 1.** (a) Downward lightning stroke to a wind turbine; (b) upward lightning initiated by a nearby CG flash; (c) upward lightning initiated by an IC flash; (d) upward lightning from a wind turbine and lightning initiated by aircraft in a winter storm (charge distribution as observed winter storms in Japan); (e) upward and downward positive flashes in the trailing stratiform of MCS; (f) repetitive corona/leader emissions from wind turbines under storms. Proportions in these diagrams are not to scale.

van der Velde et al., 2010; Montanyà et al., 2011). These intense positive CG flashes can transfer hundreds of coulombs of charge with continuing currents lasting up to tens of milliseconds (e.g., Li et al., 2008). Although downward positive flashes to wind turbines or aircraft are not common, they can induce the inception of upward flashes. However, there is significant variation from one MCS to another.

Since most of the winter lightning strikes to turbines belong to the upward lightning type (Honjo, 2015), the effect of rotation on the enhancement of lightning inception has been discussed and investigated (e.g., Rachidi et al., 2008; Wang et al., 2008; Montanyà et al., 2014a; Radičević et al., 2012). However, there is no clear evidence that the number of lightning flashes increases significantly with the effect of rotation. In the studies by Wang et al. (2008) and Wang and Takagi (2011) in Japan, the authors noted slightly larger number of strikes to rotating wind turbines than to a nearby protecting tall tower. Recently Montanyà et al. (2014a) showed corona/leader activity associated with rotating wind turbines (Fig. 1f). This activity can last for more than an hour, especially when the turbines are under an electrically charged stratiform region. This activity, even if it may not result in a

complete lightning flash, can stress the dielectric properties of blades and needs to be considered in lightning protection standards.

In the case of aircraft, Fig. 1d would correspond to those cases of encounters between aircraft and lightning or the cases of lightning initiated by the aircraft. There is no information about the occurrence of lightning that is initiated by the aircraft but induced by another lightning flash (Fig. 1b and c). Initiation by aircraft can be more efficient when thundercloud charges are closer to the ground and charge may be larger because of less frequent discharging by lightning. That is the case of winter thunderstorms (Fig. 1d) and also the conditions under stratiform regions of MCSs (Fig. 1e and f). The situation in Fig. 1e also happens to aircraft where continuous corona discharges without resulting in lightning. Montanyà et al. (2014a) showed an example.

### 3 Winter thunderstorms and global winter lightning

#### 3.1 Meteorology of winter thunderstorm areas

Thunderstorms develop as convective clouds to altitudes where it is cold enough for graupel and ice crystals to form and separate, creating layers of opposite cloud charges. Their development depends on the presence of conditional stability, with temperatures decreasing with height over a large depth of the troposphere (steep lapse rates), while the boundary layer must contain sufficient amounts of water vapor whose latent energy is released in ascending parcels, causing positive buoyancy (see Wallace and Hobbs, 2006). In summer, water vapor is supplied by large evapotranspiration while diurnal heating is strong enough over land to create the needed vertical temperature gradients, often with help from the dynamics within low-pressure systems. Convergence and ascending air near the surface is required to carry parcels to their level of free convection.

In the winter period, diurnal heating is weak and moisture content is much reduced over land. Low-pressure systems are more vigorous and bring cold air masses from polar and arctic regions southward to midlatitudes, creating strong vertical temperature gradients as cold continental air flows over relatively warm seas and ocean currents. Air parcels near the surface then experience no inhibiting warm layers on their way to the equilibrium level, often the tropopause, and occur over large regions over sea behind cold fronts. The tropopause is found between 10 and 15 km at midlatitudes in summer but can descend to 5–10 km in winter, limiting the vertical extent of convection. Just as in summer, low-level convergent winds organize the triggering of storms, but over sea these are often found near upwind coastlines, where enhanced friction and sloping terrain creates a relative stagnation and ascending flow.

### 3.1.1 Japan

In the Northern Hemisphere, a well-known area of winter storms is found in Japan. There, three types of winter thunderstorms are identified in Adachi et al. (2005): thunderstorms associated with cold fronts crossing the Sea of Japan, thunderstorms systems originating in low-pressure areas over the Pacific Ocean and thunderstorms originating in the Japan Sea Polar Air Mass Convergence Zone (JPCZ). The storms originating in the JPCZ are due to advection of dry and cold air masses from the Eurasian continent. The interaction of these cold and dry air masses over the Sea of Japan leads to increases in the water vapor content by evaporation. Arriving on the Japan mainland, convergence with horizontal winds due to topographic effects produces strong updrafts supporting the formation of thunderstorms. A fourth type of winter thunderstorms is described by Sugita and Matsui (2008). This type corresponds to isolated storms, which might significantly contribute to the number of winter thunderstorm days. Winter storms in Japan are known for the high occurrence of positive lightning compared to negative and bipolar lightning (e.g., Wu et al., 2014). This situation results in energetic lightning in terms of total charge transfer and the numerous damages to wind turbines (Yokoyama et al., 2014; Honjo, 2015).

### 3.1.2 Europe

In Europe, the prevailing Icelandic low and the Azores high-pressure systems can produce intense low-pressure systems developing over the warm Gulf Stream (e.g., Holley et al., 2014). The largest amplitude systems transport cold unstable arctic air masses into western Europe at their rear side and often stagnate in the area of the Mediterranean Sea, forming Genoa lows with a high number of fall/winter thunderstorms. In mid-winter, stable cold continental air masses over central Europe via the Balkans and France may also slide into the Mediterranean and produce shallow winter thunderstorms over the prevalent warm water there. Estofex (<http://www.estofex.org/>) provides a comprehensive archive of thunderstorms, including winter.

### 3.1.3 North America

In the United States, large winter depressions develop over the Gulf Stream and move north along the eastern coast (e.g., Dirks et al., 1988) before reaching Canada. The energy to feed these storms originates in the air–sea interaction from the warm Gulf Stream water and baroclinic instability within the cold air mass over the continent. Blizzards form over the northeastern USA and thunderstorms are produced as the cold front and cold continental air masses flow out over the Great Lakes (with lake effect snow) and the warm Gulf Stream, where the cold front collides with warm subtropical air, producing linear thunderstorm systems. The west

coast of the continent experiences similar conditions as western Europe, with cold unstable maritime air masses reaching mainly the shores of western Canada where lifting by the Rocky Mountains can initiate electrified convection.

Another cause of winter storms in Canada and the central USA are outbreaks of Arctic fronts (e.g., Holle and Watson, 1996) in which cold Arctic air masses move from north to south, meeting warm humid air from the Gulf of Mexico. Along these cold fronts thunderstorms are formed in the warm elevated layer, producing frozen precipitation at the surface.

### 3.1.4 General effect of ocean gyres

Every major ocean basin (North Atlantic, North Pacific, South Atlantic, South Pacific, etc.) contains a basin-scale rotating current flow – a gyre – with clockwise (counterclockwise) rotation in the Northern (Southern) Hemisphere (Fig. 2). The primary drive for these gyres is the zonal wind stress from prevailing easterly winds in the tropics – otherwise known as the trade winds. In this near-equatorial portion of the gyre, the ocean surface is warmed substantially by sunlight; at the western limit of this equatorial transit, this warm oceanic flow is diverted northward and southward, depending on hemisphere. Since the surface air over continents is increasingly colder away from the Equator and tends to be moving eastward off the continents at midlatitude, warm ocean water in this poleward current is found consistently in all gyres beneath colder air away from the Equator. This configuration is inherently unstable and can produce vigorous atmospheric convection and thunderstorm activity. The Gulf Stream along the North American coast and the Kuroshio Current along the eastern coast of Asia (China, Japan, Korea and Russia) are prime examples in which lightning activity over warm ocean water is prevalent during winter. In contrast, the return current on the eastern boundaries of oceanic gyres, and moving equatorward, is colder than the air overlying it. This situation is stable against convection and lightning is absent. A prime example is the Eastern Pacific Ocean. Similar behavior is present in the gyres of the Southern Hemisphere.

## 3.2 Global maps of winter lightning

In this section, we present maps of global winter thunderstorms that are useful for risk assessment. As already mentioned at the introduction, we will refer to those thunderstorms occurring in cold air masses and not necessarily in the corresponding winter season as winter thunderstorms. In order to process the maps we used a simple criterion to define winter lightning conditions: temperatures equal or lower than  $-10^{\circ}\text{C}$  at the 700 hPa level ( $\sim 3$  km above mean sea level). This criterion matches the observations by Montanyà et al. (2007), Saito et al. (2012) and Warner et al. (2014) for the analyzed winter flashes and thunderstorms. Temperature

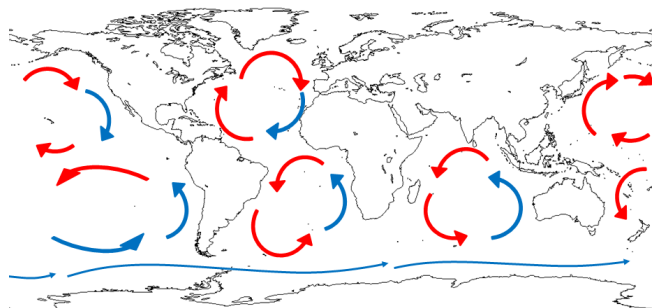


**Figure 2.** Simplified distribution of the most significant rotating oceanic currents: North Atlantic Gyre, South Atlantic Gyre, North Pacific Gyre, South Pacific Gyre, Indian Ocean Gyre and the Antarctic Circumpolar Gyre (for more information see Siedler et al., 2013). Red and blue arrows indicate warm and cold currents, respectively.

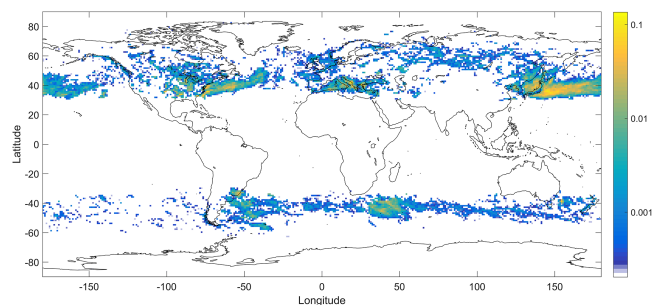


**Figure 3.** Global distribution of winter lightning stroke density (strokes  $\text{km}^{-2} \text{yr}^{-1}$ ) for the period 2009–2013.

data at this pressure level are obtained on a  $1^\circ \times 1^\circ$  grid from ECMWF Re-Analysis (ERA-Interim). Global lightning data were provided by the World Wide Lightning Location Network (WWLLN) (Rodger et al., 2006). The period of analysis correspond to 5 years (2009–2013). The results are presented in three maps: average annual stroke density, seasonal variation of the lightning stroke density and average number of winter thunderstorms per year.

Figure 3 displays the global winter lightning distribution. The maximum annual stroke density was found to be no higher than  $0.5 \text{ strokes km}^{-2} \text{yr}^{-1}$ ; in order to present a more clear map, Fig. 3 has been limited to  $0.2 \text{ strokes km}^{-2} \text{yr}^{-1}$ .

The map in Fig. 3 clearly shows the previously discussed areas of winter lightning (Japan, east of USA, Mediterranean) and other areas with wind farms such as Uruguay and surroundings, southwest of the Indian Ocean and Tasmanian Sea. Figure 4 plots the seasonal variation of the global winter lightning activity. In this case, each grid cell corresponds to the 5-year average value of the number of strokes divided by the cell area for the corresponding period.

The average stroke densities shown in the maps in Figs. 3 and 4 are influenced by the detection efficiency of the WWLLN. As with any long-range VLF lightning location

system, WWLLN has a detection efficiency for each location that changes during the hours of the day due to VLF wave propagation, as well as during time due to network upgrades, sensitivity of the sensors and data processing methods. The estimated overall stroke detection efficiency of WWLLN is considered to be 11 % according to Hutchins et al. (2012), Abarca et al. (2010) and Rodger et al. (2009). Although the relative detection efficiency is provided periodically, we did not apply any compensation. For further information relative to the detection efficiency, see Hutchins et al. (2012). Moreover, the WWLLN makes no distinction between cloud-to-ground flashes and intra-cloud flashes. Then, the results presented in Figs. 3 and 4 are relative to WWLLN detections and cannot be adopted as absolute values.

Probably the most useful metric for evaluation of the winter lightning risk is the average number of winter thunderstorm days per year ( $T_w$ ). Here  $T_w$  is obtained in a  $1^\circ \times 1^\circ$  grid. A winter thunderstorm day in a grid cell is counted when at least one lightning stroke agreeing with the presented temperature–pressure level criterion is detected within the cell. The  $T_w$  map is depicted in Fig. 5.

## 4 Discussion

Areas of winter lightning are well defined outside the Intertropical Convergence Zone (ITCZ). The resulting maps show that contrary to what occurs with deep convective storms, winter lightning activity is more distributed over the oceans than over continental areas. One of the reasons is the role that warm oceanic water plays to produce energy for convection during cold seasons. In Fig. 2 we resumed the main oceanic current gyres. Note how this simple picture goes a long way in explaining the patterns of winter lightning in Figs. 3 and 5. The preference for oceanic and coastal areas is an important aspect for coastal onshore and offshore wind farms.

Regarding winter thunderstorm activity and risk assessment, the maps indicate some particular areas more critical to winter lightning because of prevalence in larger areas onshore in proximity to active ocean areas. The Japan mainland is surrounded by winter thunderstorms; the map in Fig. 5 shows how especially the west coast is particularly active reaching in some areas about 24 days of winter thunderstorms per year. Another particularly active region that affects extensive onshore areas is found in the Mediterranean Sea (e.g., South Italy and the Balkans). In the case of North America, the highest number of annual winter thunderstorm days per year is located in the Atlantic Ocean. Although the central eastern regions of the USA (Great Lakes) the number of winter thunderstorms per year are not so high, the lightning stroke densities are significant. Other areas sensitive to winter thunderstorms because of present installations and also ongoing offshore farms include the northern coast of Spain, western coast of France and the European coast in the

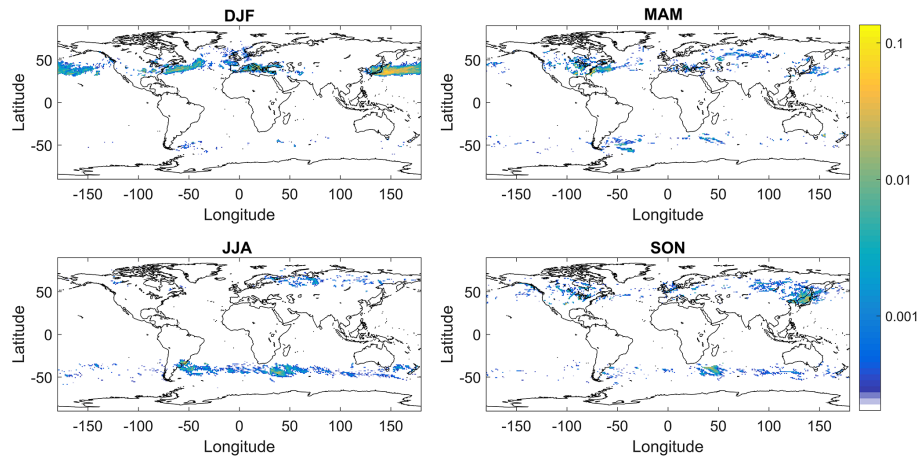


**Figure 4.** Seasonal variation of the winter lightning stroke density distribution for the period of 2009–2013. The values are calculated as the average number of strokes for the 5 years in each grid cell divided by the area of the cell. Note the major shift of activity from DJF and MAM periods in the Northern Hemisphere to more JJA and SON periods in the Southern Hemisphere.

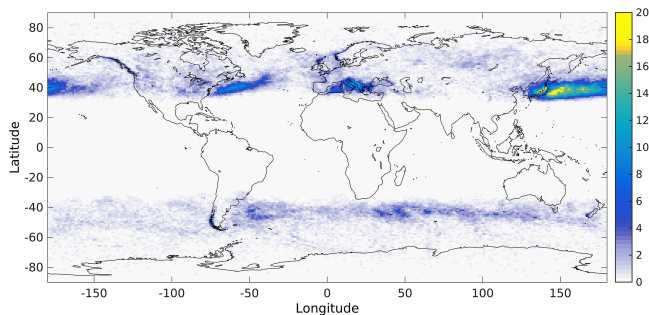


**Figure 5.** Average number of winter thunderstorm days per year ( $T_w$ ) for the period 2009–2013.

North Sea. In addition, Uruguay and its surroundings, southern New Zealand, southern west coast of Chile and Southeast Alaska must be highlighted as well.

For risk assessment it is convenient to consider the  $T_w$  provided in Fig. 5 as the first indicator of risk to winter lightning activity. In addition to identification of winter thunderstorm areas, the seasonal variation of the winter lightning activity (Fig. 4) is another aspect deserving attention for planning purposes, for equipment maintenance or to set up lightning warnings (e.g., CENELEC European standard EN 50536, 2011). That is also important when working with tall cranes. In the Northern Hemisphere the activity is concentrated from October to June whereas in the Southern Hemisphere the activity is significant from April to September.

## 5 Conclusions

Winter lightning poses a critical risk to tall objects such as wind turbines and also to flying aircraft because these have favorable conditions for self-lightning initiation. In this paper

we presented for the first time world maps with winter lightning activity. The maps show that winter lightning occurs in extratropical regions with preference for oceanic and coastal areas in the western limits of permanent oceanic gyres. As a general conclusion, winter lightning maps presented in this work suggest that winter activity in Japan may be the highest, as supported by the previously discussed works. Japan is not an exclusive region for winter lightning, as other areas such as the Mediterranean and the USA are active as well. In the Southern Hemisphere, Uruguay and its surroundings, the southwestern Indian Ocean and the Tasman Sea experience the highest activity.

The maps may be of use for risk assessment analysis such as proposed in standards (e.g., the International Electrotechnical Commission, IEC), providing a tool to identify areas of winter lightning activity. In these areas, tall structures such as wind turbines can be exposed to very energetic lightning and to an environment favorable for lightning self-initiation. Risk assessment of the effect of winter lightning shall also include the exposure. In the case of wind turbines, those turbines located in areas influenced by winter lightning at high altitudes can experience very high number of lightning flashes. Locations at the greatest risk tend to be offshore (e.g., offshore wind turbines, platforms and helicopter operations at those sites). In these situations, the installation of a tall object can significantly increase the winter lightning activity.

Finally, the simple methodology employed to classify a lightning stroke as being winter lightning may be beneficial in conducting further risk assessment based on local combined lightning and meteorological data.

*Acknowledgements.* This work was supported by research grants from the Spanish Ministry of Economy and Competitiveness (MINECO) AYA2011-29936-C05-04, (MINECO/FEDER) ESP2013-48032-C5-3-R and (MINECO/FEDER) ESP2015-

69909-C5-5-R. This work has been part of the authors' activity in the CIGRE WG C4.36 "Winter Lightning Parameters and Engineering Consequences for Wind Turbines".

Edited by: S. Tinti

Reviewed by: two anonymous referees

## References

- Abarca, S. F., Corbosiero, K. L., and Galarneau, T. J.: An evaluation of the Worldwide Lightning Location Network (WWLLN) using the National Lightning Detection Network (NLDN) as ground truth, *J. Geophys. Res.*, 115, D18206, doi:10.1029/2009JD013411, 2010.
- Adachi, T., Fukunishi, H., Takahashi, Y., Sato, M., Ohkubo, A., and Yamamoto, K.: Characteristics of thunderstorm systems producing winter sprites in Japan, *J. Geophys. Res.*, 110, D11203, doi:10.1029/2004JD005012, 2005.
- Anderson, G. and Klugmann, D.: A European lightning density analysis using 5 years of ATDnet data, *Nat. Hazards Earth Syst. Sci.*, 14, 815–829, doi:10.5194/nhess-14-815-2014, 2014.
- CENELEC: Protection against lightning – thunderstorm warning systems, European Standard, EN 50536, 2011.
- Bazelyan, E. M. and Raizer, Y. P.: *Spark Discharge*, CRC Press Inc., 206 pp., 1998.
- Bech, J., Pineda, N., Rigo, T., and Aran, M.: Remote sensing analysis of a Mediterranean thundersnow and low-altitude heavy snowfall event, *Atmos. Res.*, 123, 305–322, 2013.
- Dirks, R. A., Kuettner, J. P., and Moore, J. A.: Genesis of Atlantic Lows Experiment (GALE): An overview, *B. Am. Meteor. Soc.*, 69, 148–160, 1988.
- Gough, W. R., Hemink, J., Niemeijer, S., and Fahey, T. H.: The prediction and occurrence of aircraft lightning encounters at Amsterdam-Schiphol Airport, in *Proc. 47th AIAA Aerospace Sciences Meeting*, 2009.
- Holle, R. L. and Watson, A. I.: Lightning during Two Central U.S. Winter Precipitation Events, *Weather Forecast.*, 11, 599–614, 1996.
- Holley, S. M., Dorling, S. R., Steele, C. J., and Earl, N.: A climatology of convective available potential energy in Great Britain, *Int. J. Climatol.*, 34, 3811–3824, 2014.
- Honjo, N.: Risk and its reduction measure for wind turbine against the winter lightning, in *Proc. Asia-Pacific Intl. Conf. on Lightning*, Nagoya, Japan, 2015, 665–670, 2015.
- Hunter, S. M., Underwood, S. J., Holle, R. L., and Mote, T. L.: Winter lightning and heavy frozen precipitation in the southeast United States, *Weather Forecast.*, 16, 478–490, 2001.
- Hutchins, M. L., Holzworth, R. H., Brundell, J. B., and Rodger, C. J.: Relative detection efficiency of the world wide lightning location network, *Radio Sci.*, 47, RS6005, doi:10.1029/2012RS005049, 2012.
- Li, J., Cummer, S. A., Lyons, W. A., and Nelson, T. E.: Coordinated analysis of delayed sprites with high speed images and remote electromagnetic fields, *J. Geophys. Res.*, 113, D20206, doi:10.1029/2008JD010008, 2008.
- López, J., Montanyà, J., Maruri, M., De la Vega, D., Aranda, J. A., and Gaztelumendi, S.: Lightning initiation from a tall structure in the Basque Country, *Atmos. Res.*, 117, 28–36, 2012.
- Lyons, W. A.: Sprite observations above the U.S. High Plains in relation to their parent thunderstorm systems, *J. Geophys. Res.*, 101, 29641–29652, 1996.
- Krehbiel, P. R., Rioussset, J. A., Pasko, V. P., Thomas, R. J., Rison, W., Stanley, M. A., and Edens, H. E.: Upward electrical discharges from thunderstorms, *Nature Geosci.*, 1, 233–237, 2008.
- MacGorman, D. and Morgenstern, C. D.: Some characteristics of cloud to ground lightning in mesoscale convective systems, *J. Geophys. Res.*, 103, 14011–14023, 1998.
- Michimoto, K.: A study of radar echoes and their relation to lightning discharges of thunderclouds in the Hokuriku district. II: Observation and analysis of "single-flash" thunderclouds in mid-winter, *J. Meteorol. Soc. Jpn.*, 71, 195–204, 1993.
- Montanyà, J., Soula, S., Diendorfer, G., Solà, G., and Romero, D.: Analysis of the altitude of the isotherms and the electrical charge for flashes that struck the Gaisberg tower, *Proc. Intl. Conf. on Atmospheric Electricity*, Beijing, China, 2007.
- Montanyà, J., Fabró, F., van der Velde, O., and Hermoso, B.: Sprites and Elves as proxy of energetic lightning flashes in winter. What can we learn from mesospheric discharges for the protection of wind turbines?, *Proc. Intl. Symp. on Winter Lightning*, ISWL 2011, Sapporo, Japan, 2011.
- Montanyà, J., van der Velde, O., and Williams, E. R.: Lightning discharges produced by wind turbines, *J. Geophys. Res. Atmos.*, 119, 1455–1462, 2014a.
- Montanyà, J., Fabró, F., van der Velde, O., Romero, D., Solà, G., Hermoso, J. R., Soula, S., Williams, E. R., and Pineda, N.: Registration of X-rays at 2500 m altitude in association with lightning flashes and thunderstorms, *J. Geophys. Res. Atmos.*, 119, 1492–1503, 2014b.
- Murooka, Y.: A Survey of Lighting Interaction with Aircraft in Japan, *Res. Lett. Atmos. Electricity*, 2, 101–106, 1992.
- Poelman, D. R., Schulz, W., Diendorfer, G., and Bernardi, M.: The European lightning location system EUCLID – Part 2: Observations, *Nat. Hazards Earth Syst. Sci.*, 16, 607–616, doi:10.5194/nhess-16-607-2016, 2016.
- Rachidi, F., Rubinstein, M., Montanyà, J., Bermudez, J. L., Rodriguez, R., Solà, G., and Korovkin, N.: Review of current issues in lightning protection of new generation wind turbine blades, *IEEE Trans. Ind. Electron.*, 55, 2489–2496, 2008.
- Radičević, R. M., Savic, M. S., Madsen, S. F., and Badea, I.: Impact of wind turbine blade rotation on the lightning strike incidence – A theoretical and experimental study using a reduced-size model, *Energy*, 45, 644–654, 2012.
- Rodger, C. J., Werner, S., Brundell, J. B., Lay, E. H., Thomson, N. R., Holzworth, R. H., and Dowden, R. L.: Detection efficiency of the VLF World-Wide Lightning Location Network (WWLLN): initial case study, *Ann. Geophys.*, 24, 3197–3214, 2006.
- Rodger, C. J., Brundell, J. B., Holzworth, R. H., Lay, E. H., Crosby, N. B., Huang, T.-Y., and Rycroft, M. J.: Growing detection efficiency of the world wide lightning location network, *AIP Conference Proceedings*, 1118, 15–20, doi:10.1063/1.3137706, 2009.
- Saito, M., Ishii, M., Fujii, F., and Matsui, M.: Seasonal Variation of Frequency of High Current Lightning Discharges Observed by JLDN, *IEEJ Trans. P & E*, 132, 536–541, 2012.
- Saunders, C. P. R., Bax-Norman, H., Emersic, C., Avila, E. E., and Castellano, N. E.: Laboratory studies of the effect of cloud conditions on graupel/crystal charge transfer in thunderstorm electrification, *Q. J. Roy. Meteor. Soc.*, 132, 2653–2674, 2006.

- Siedler, G., Griffies, S. M., Gould, J., and Church, J. A. (Eds.): Ocean Circulation and Climate A 21st century perspective. International geophysics series, p. 103, Amsterdam Academic Press, 2013.
- Sugita, A., Matsui, M.: Examples of winter lightning observed by the JLDN, in Proc. of 2008 ILDC/ILMC, Tucson, Arizona, 2008.
- Takahashi, T.: Thunderstorm electrification-A numerical study, *J. Atmos. Sci.*, 41, 2541–2558, 1984.
- van der Velde, O. A., Montanyà, J., Soula, S., Pineda, N., and Bech, J.: Spatial and temporal evolution of horizontally extensive lightning discharges associated with sprite-producing positive cloud-to-ground flashes in northeastern Spain, *J. Geophys. Res.*, 115, A00E56, doi:10.1029/2009JA014773, 2010.
- Wallace, J. M. and Hobbs, P. V.: Atmospheric science: An introductory survey. 2nd Ed., Academic Press, 345–346, 2006.
- Wang, D. and Takagi, N.: Typical characteristics of upward lightning observed in Japanese winter Thunderstorms and Their Physical Implications, in Proc. Intl. Conf. on Atmospheric Electricity, 2011.
- Wang, D., Takagi, N., Watanabe, T., Sakurano, N., and Hashimoto, M.: Observed characteristics of upward leaders that are initiated from a windmill and its lightning protection tower, *Geophys. Res. Lett.*, 35, L02803, doi:10.1029/2007GL032136, 2008.
- Warner, T. A., Cummins, K. L., and Orville, R. E.: Upward lightning observations from towers in Rapid City, South Dakota and comparison with National Lightning Detection Network data, 2004–2010, *J. Geophys. Res.*, 117, D19109, doi:10.1029/2012JD018346, 2012.
- Warner, T. A., Lang, T. J., and Lyons, W. A.: Synoptic scale outbreak of self-initiated upward lightning (SIUL) from tall structures during the central U.S. blizzard of 1–2 February 2011, *J. Geophys. Res.-Atmos.*, 119, 9530–9548, 2014.
- Wilkinson, J. M., Wells, H., Field, P. R., and Agnew, P.: Investigation and prediction of helicopter-triggered lightning over the North Sea, *Met. Apps*, 20, 94–106, 2013.
- Williams, E. R.: The tripole structure of thunderstorms, *J. Geophys. Res.*, 94, 13151–13167, 1989.
- Williams, E. R., Lyons, W. A., Hobara, Y., Mushtak, V. C., Asencio, N., Boldi, R., Bór, J., Cummer, S. A., Greenberg, E., Hayakawa, M., Holzworth, R. H., Kotroni, V., Li, J., Morales, C., Nelson, T. E., Price, C., Russell, B., Sato, M., Satori, G., Shirahata, K., Takahashi, Y., and Yamashita, K.: Ground-based detection of sprites and their parent lightning flashes over Africa during the 2006 AMMA campaign, *Q. J. Roy. Meteorol. Soc.*, 136, 257–271, 2010.
- Wu, T., Yoshida, S., Ushio, T., Kawasaki, Z., Takayanagi, Y., and Wang, D.: Large bipolar lightning discharge events in winter thunderstorms in Japan, *J. Geophys. Res.-Atmos.*, 119, 555–566, 2014.
- Yokoyama, Y., Hermoso, B., Cooray, V., D'Alessandro, F., Dendorfer, G., Duquerroy, P., Engmann, G., Erichsen, H., Galvan, A., Gockenbach, E., Havelka, M., Ishii, M., Kanashiro, A., Méndez, M., Montanya, J., Paolone, M., Rachidi, F., Rousseau, A., Sekioka, S., Shindo, T., Torres, H., Tudor, L., Yamamoto, K., and Yasuda, Y.: Lightning protection of wind turbine blades, *Electra*, 274, 43–45, 2014.